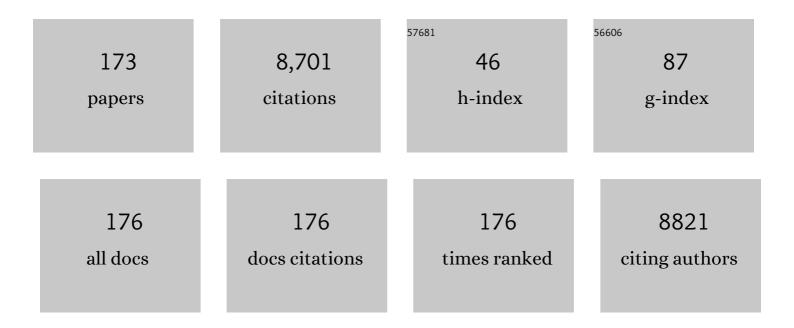
Jianming Zhang

List of Publications by Year in descending order

Source: https://exaly.com/author-pdf/2515539/publications.pdf Version: 2024-02-01



#	Article	IF	CITATIONS
1	Efficient transition metal dichalcogenides exfoliation by cellulose nanocrystals for ultrabroad-pH/temp stable aqueous dispersions and multi-responsive photonic films. Chemical Engineering Journal, 2022, 428, 132594.	6.6	16
2	Guiding cellular channels of artificial nanohybrid woods for anisotropic properties and solar-thermal evaporation. Chemical Engineering Journal, 2022, 428, 132060.	6.6	13
3	Ultrasonication pretreatment assisted rapid co-assembly of cellulose nanocrystal and metal ion for multifunctional application. Carbohydrate Polymers, 2022, 277, 118829.	5.1	6
4	Distinct liquid crystal self-assembly behavior of cellulose nanocrystals functionalized with ionic liquids. Colloids and Surfaces A: Physicochemical and Engineering Aspects, 2022, 632, 127790.	2.3	9
5	Melt-processed poly (L-lactic acid) / cellulose nanocrystals biocomposites for 3D printing: Improved melt processibility and inter-fuse adhesion. Composites Science and Technology, 2022, 218, 109135.	3.8	20
6	Biomass vs inorganic and plastic-based aerogels: Structural design, functional tailoring, resource-efficient applications and sustainability analysis. Progress in Materials Science, 2022, 125, 100915.	16.0	73
7	Facile fabrication of high nanofiller-content natural rubber nanocomposites for reversible plasticity shape memory polymers. Composites Science and Technology, 2022, 221, 109349.	3.8	8
8	Rational design of POSS containing low dielectric resin for SLA printing electronic circuit plate composites. Composites Science and Technology, 2022, 223, 109403.	3.8	32
9	Upgrading the Pyrolysis Carbon Black from Waste Tire by Hybridization with Cellulose. Industrial & Engineering Chemistry Research, 2022, 61, 6512-6520.	1.8	5
10	Rapidly regenerated CNC/TiO2/MnO2 porous microspheres for high-efficient dye removal. Carbohydrate Polymers, 2022, 292, 119644.	5.1	10
11	Cellulose nanocrystal enhanced, high dielectric 3D printing composite resin for energy applications. Composites Science and Technology, 2022, 227, 109601.	3.8	19
12	Facile in-situ growth of metal–organic framework layer on carboxylated nanocellulose/chitosan aerogel spheres and their high-efficient adsorption and catalytic performance. Applied Surface Science, 2022, 599, 153974.	3.1	12
13	Effects of epoxy resin crosslinking networks on stereocomplexation of poly(<scp>l</scp> â€lactic) Tj ETQq1 1 0.	784314 rg 1.6	;BT ₃ /Overloc
14	Designs of conductive polymer composites with exceptional reproducibility of positive temperature coefficient effect: A review. Journal of Applied Polymer Science, 2021, 138, 49677.	1.3	26
15	Dependence of microstructure and properties of polypropylene/bromoâ€isobutyleneâ€isoprene rubber thermoplastic vulcanizates on the molding process. Journal of Applied Polymer Science, 2021, 138, 49659.	1.3	3
16	Design and Fabrication of the Evolved Zeolitic Imidazolate Framework-Modified Polylactic Acid Nonwoven Fabric for Efficient Oil/Water Separation. ACS Applied Materials & Interfaces, 2021, 13, 14653-14661.	4.0	28
17	Natural Rubber Latex Reinforced by Graphene Oxide/Zwitterionic Chitin Nanocrystal Hybrids for High-Performance Elastomers without Sulfur Vulcanization. ACS Sustainable Chemistry and Engineering, 2021, 9, 6470-6478.	3.2	13
18	Effects of cellulose nanocrystals on the vulcanization of natural rubber/cellulose nanocrystals nanocomposite and corresponding regulating strategies. Journal of Polymer Science, 2021, 59, 2990-3000.	2.0	4

#	Article	IF	CITATIONS
19	Green fabrication of porous microspheres containing cellulose nanocrystal/MnO2 nanohybrid for efficient dye removal. Carbohydrate Polymers, 2021, 270, 118340.	5.1	17
20	Inserting insulating barriers into conductive particle channels: A new paradigm for fabricating polymer composites with high dielectric permittivity and low dielectric loss. Composites Science and Technology, 2021, 216, 109070.	3.8	27
21	High-yield, high-conductive graphene/nanocellulose hybrids prepared by Co-exfoliation of low-oxidized expanded graphite and microfibrillated cellulose. Composites Part B: Engineering, 2021, 225, 109250.	5.9	13
22	Polymer grafting on cellulose nanocrystals initiated by ceric ammonium nitrate: is it feasible under acid-free conditions?. Green Chemistry, 2021, 23, 8581-8590.	4.6	15
23	Carboxylation of Cellulose Nanocrystals for Reinforcing and Toughing Rubber Through Dual Cross-linking Networks. ACS Applied Polymer Materials, 2021, 3, 6120-6129.	2.0	12
24	Biomimetic Hybridization of Janus-like Graphene Oxide into Hierarchical Porous Hydrogels for Improved Mechanical Properties and Efficient Solar Desalination Devices. ACS Nano, 2021, 15, 19877-19887.	7.3	76
25	Modified ammonium persulfate oxidations for efficient preparation of carboxylated cellulose nanocrystals. Carbohydrate Polymers, 2020, 229, 115572.	5.1	57
26	One-pot preparation of zwitterionic graphene nanosheets with exceptional redispersibility and its application in pickering emulsions. Carbon, 2020, 157, 448-456.	5.4	9
27	Air-dried porous powder of polymethyl methacrylate modified cellulose nanocrystal nanocomposite and its diverse applications. Composites Science and Technology, 2020, 188, 107985.	3.8	22
28	Tough, Ultralight, and Water-Adhesive Graphene/Natural Rubber Latex Hybrid Aerogel with Sandwichlike Cell Wall and Biomimetic Rose-Petal-Like Surface. ACS Applied Materials & Interfaces, 2020, 12, 1378-1386.	4.0	34
29	Fabricating 3D printable BIIR/PP TPV via masterbatch and interfacial compatibilization. Composites Part B: Engineering, 2020, 199, 108220.	5.9	22
30	Ionic Liquids Grafted Cellulose Nanocrystals for High-Strength and Toughness PVA Nanocomposite. ACS Applied Materials & Interfaces, 2020, 12, 38796-38804.	4.0	30
31	Design and optimization of asymmetric supercapacitors assembled by Platanus acerifolia seeds and ZIF-67 as precursors. Journal of Electroanalytical Chemistry, 2020, 878, 114668.	1.9	1
32	Facile fabrication of carboxylated cellulose nanocrystal–MnO2 beads for high-efficiency removal of methylene blue. Cellulose, 2020, 27, 7053-7066.	2.4	17
33	Origin of vacuum-assisted chiral self-assembly of cellulose nanocrystals. Carbohydrate Polymers, 2020, 245, 116459.	5.1	30
34	In-situ preparation of hollow cellulose nanocrystals/zeolitic imidazolate framework hybrid microspheres derived from Pickering emulsion. Journal of Colloid and Interface Science, 2020, 572, 160-169.	5.0	27
35	Electric Field-Induced Assembly and Alignment of Silver-Coated Cellulose for Polymer Composite Films with Enhanced Dielectric Permittivity and Anisotropic Light Transmission. ACS Applied Materials & Interfaces, 2020, 12, 24242-24249.	4.0	41
36	Janus-like asymmetrically oxidized graphene: Facile synthesis and distinct liquid crystal alignment at the oil/water interface. Carbon, 2020, 161, 316-322.	5.4	11

#	Article	IF	CITATIONS
37	Natural rubber bio-nanocomposites reinforced with self-assembled chitin nanofibers from aqueous KOH/urea solution. Carbohydrate Polymers, 2019, 225, 115230.	5.1	33
38	Synergistic effect of conductive carbon black and silica particles for improving the pyroresistive properties of high density polyethylene composites. Composites Part B: Engineering, 2019, 178, 107465.	5.9	29
39	Flash DSC study on the annealing behaviors of poly(l-lactide acid) crystallized in the low temperature region. Polymer, 2019, 174, 123-129.	1.8	14
40	Investigation of crystallization behavior of asymmetric PLLA/PDLA blend using Raman Imaging measurement. Polymer, 2019, 172, 1-6.	1.8	32
41	Recent advances in vacuum assisted self-assembly of cellulose nanocrystals. Current Opinion in Solid State and Materials Science, 2019, 23, 142-148.	5.6	19
42	Small- and wide-angle X-ray scattering study on α′-to-α transition of Poly(L-lactide acid) crystals. Polymer, 2019, 167, 122-129.	1.8	17
43	Anti-blooming effect of graphene oxide on natural rubber latex composite films. Composites Science and Technology, 2019, 174, 142-148.	3.8	12
44	Study on thermal behavior of regenerated micro-crystalline cellulose containing slight amount of water induced by hydrogen-bonds transformation. Polymer, 2019, 185, 121989.	1.8	11
45	Effect of surface chemistry on the dispersion and pH-responsiveness of chitin nanofibers/ natural rubber latex nanocomposites. Carbohydrate Polymers, 2019, 207, 555-562.	5.1	16
46	Ultralight, Superelastic, and Fatigue-Resistant Graphene Aerogel Templated by Graphene Oxide Liquid Crystal Stabilized Air Bubbles. ACS Applied Materials & Interfaces, 2019, 11, 1303-1310.	4.0	68
47	Ultrafine and carboxylated β-chitin nanofibers prepared from squid pen and its transparent hydrogels. Carbohydrate Polymers, 2019, 211, 118-123.	5.1	27
48	Simultaneous improvement of thermal stability and redispersibility of cellulose nanocrystals by using ionic liquids. Carbohydrate Polymers, 2018, 186, 252-259.	5.1	31
49	One-pot synthesis of graphene/chitin nanofibers hybrids and their remarkable reinforcement on Poly(vinyl alcohol). Carbohydrate Polymers, 2018, 194, 146-153.	5.1	26
50	Hierarchically Porous Graphene/ZIF-8 Hybrid Aerogel: Preparation, CO ₂ Uptake Capacity, and Mechanical Property. ACS Applied Materials & Interfaces, 2018, 10, 827-834.	4.0	70
51	Flexible and Tailorable Alkylviologen/Cellulose Nanocrystals Composite Films for Sustainable Applications in Electrochromic Devices. ChemElectroChem, 2018, 5, 1407-1414.	1.7	10
52	Nitrogen-Enriched Carbon Nanofiber Aerogels Derived from Marine Chitin for Energy Storage and Environmental Remediation. ACS Sustainable Chemistry and Engineering, 2018, 6, 177-185.	3.2	83
53	Green Fabrication of Regenerated Cellulose/Graphene Films with Simultaneous Improvement of Strength and Toughness by Tailoring the Nanofiber Diameter. ACS Sustainable Chemistry and Engineering, 2018, 6, 1271-1278.	3.2	39
54	Influence of Branched Polyester Chains on the Emission Behavior of Dipyridamole Molecule and Its Biosensing Ability. ACS Omega, 2018, 3, 15530-15537.	1.6	4

#	Article	IF	CITATIONS
55	Study on the impact of graphene and cellulose nanocrystal on the friction and wear properties of SBR/NR composites under dry sliding conditions. Wear, 2018, 414-415, 43-49.	1.5	22
56	Study on phase transition behavior and lamellar orientation of uniaxially stretched poly(ÊŸ-lactide) / cellulose nanocrystal-graft-poly(d-lactide) blend. Polymer, 2018, 150, 184-193.	1.8	8
57	Rotationâ€essisted formation of poly(3â€butylthiophene) nanowires: Morphology, microstructure, and electrical property. Journal of Polymer Science, Part B: Polymer Physics, 2018, 56, 1027-1034.	2.4	0
58	One-Pot Preparation of Carboxylated Cellulose Nanocrystals and Their Liquid Crystalline Behaviors. ACS Sustainable Chemistry and Engineering, 2018, 6, 12403-12410.	3.2	70
59	Green and facile surface modification of cellulose nanocrystal as the route to produce poly(lactic) Tj ETQq1 1 0.7	84314 rgB	BT /Overlock
60	Modifying Mechanical, Optical Properties and Thermal Processability of Iridescent Cellulose Nanocrystal Films Using Ionic Liquid. ACS Applied Materials & Interfaces, 2017, 9, 3085-3092.	4.0	97
61	Distribution of Polymorphic Crystals in the Ring-Banded Spherulites of Poly(butylene adipate) Studied Using High-Resolution Raman Imaging. Macromolecules, 2017, 50, 3377-3387.	2.2	18
62	Phase Transition Mechanism of Poly(<scp>l</scp> -lactic acid) among the α, Î′, and β Forms on the Basis of the Reinvestigated Crystal Structure of the β Form. Macromolecules, 2017, 50, 3285-3300.	2.2	53
63	Temperature-Dependent Recrystallization Morphologies of Carbon-Coated Isotactic Polypropylene Highly Oriented Thin Films. Macromolecules, 2017, 50, 3582-3589.	2.2	24
64	Improved processability and performance of biomedical devices with poly(lactic acid)/poly(ethylene) Tj ETQqO 0 () rgBT /Ove	erlock 10 Tf 5 15
65	Main chain copolysiloxanes with terthiophene and perylenediimide units: synthesis, characterization and electrical memory. Polymer Chemistry, 2017, 8, 3515-3522.	1.9	6
66	Graphene/cellulose nanocrystals hybrid aerogel with tunable mechanical strength and hydrophilicity fabricated by ambient pressure drying technique. RSC Advances, 2017, 7, 16467-16473.	1.7	35
67	Enhanced Toughness and Thermal Stability of Cellulose Nanocrystal Iridescent Films by Alkali Treatment. ACS Sustainable Chemistry and Engineering, 2017, 5, 8951-8958.	3.2	85
68	High-yield preparation of a zwitterionically charged chitin nanofiber and its application in a doubly pH-responsive Pickering emulsion. Green Chemistry, 2017, 19, 3665-3670.	4.6	78
69	Diameter and thermal treatment dependent structure and optical properties of poly(3-hexylthiophene) nanotubes. Journal of Materials Chemistry C, 2017, 5, 8315-8322.	2.7	12
70	Multiple Chain Packing and Phase Composition in Regioregular Poly(3-butylthiophene) Films. Macromolecules, 2016, 49, 9493-9506.	2.2	17
71	ZIF-8@Polyvinylpyrrolidone Nanocomposites Based N-Doped Porous Carbon for Highly Efficient Oxygen Reduction Reaction in Alkaline Solution. Journal of the Electrochemical Society, 2016, 163, H459-H464.	1.3	19
72	Dependence of poly(3-hydroxybutyrate) crystal modifications on film thickness as revealed by reflection-absorption infrared spectroscopy. Vibrational Spectroscopy, 2016, 86, 35-39.	1.2	4

#	Article	IF	CITATIONS
73	Iridescent graphene/cellulose nanocrystal film with water response and highly electrical conductivity. RSC Advances, 2016, 6, 93673-93679.	1.7	24
74	Higher-order structure formation of a poly(3-hydroxybutyrate) film during solvent evaporation. RSC Advances, 2016, 6, 95021-95031.	1.7	3
75	Controllable lateral contraction and mechanical performance of chemically reduced graphene oxide paper. Carbon, 2016, 107, 46-55.	5.4	17
76	Graphene oxide/cellulose composite films with enhanced UV-shielding and mechanical properties prepared in NaOH/urea aqueous solution. RSC Advances, 2016, 6, 73358-73364.	1.7	35
77	Role of Dicumyl Peroxide on Toughening PLLA via Dynamic Vulcanization. Industrial & Engineering Chemistry Research, 2016, 55, 9907-9914.	1.8	14
78	Effect of morphology designing on the structure and properties of PLA/PEG/ABS blends. Colloid and Polymer Science, 2016, 294, 1779-1787.	1.0	14
79	Synthesis and characterization of cellulose nanocrystal-graft-poly(d-lactide) and its nanocomposite with poly(l-lactide). Polymer, 2016, 103, 365-375.	1.8	55
80	Preparation of poly(3-butylthiophene) form II crystal by low-temperature aging and a proposal for form II-to-form I transition mechanism. Polymer, 2016, 105, 88-95.	1.8	7
81	Pulsed Electric Fields on Poly- <scp>l</scp> -(lactic acid) Melt Electrospun Fibers. Industrial & Engineering Chemistry Research, 2016, 55, 7116-7123.	1.8	25
82	Hierarchically Porous N-doped Carbon Derived from ZIF-8 Nanocomposites for Electrochemical Applications. Electrochimica Acta, 2016, 196, 699-707.	2.6	182
83	Study on π–π Interaction in H- and J-Aggregates of Poly(3-hexylthiophene) Nanowires by Multiple Techniques. Journal of Physical Chemistry B, 2015, 119, 8446-8456.	1.2	43
84	Cell Morphology and Improved Heat Resistance of Microcellular Poly(<scp>l</scp> -lactide) Foam via Introducing Stereocomplex Crystallites of PLA. Industrial & Engineering Chemistry Research, 2015, 54, 2476-2488.	1.8	59
85	Effect of a small amount of sulfur on the physical and mechanical properties of peroxideâ€cured fully saturated <scp>HNBR</scp> compounds. Journal of Applied Polymer Science, 2015, 132, .	1.3	8
86	Effect of mold temperature on the structures and mechanical properties of micro-injection molded polypropylene. Materials and Design, 2015, 88, 245-251.	3.3	37
87	Effect of cellulose solubility on the thermal and mechanical properties of regenerated cellulose/graphene nanocomposites based on ionic liquid 1-allyl-3-methylimidazoliun chloride. RSC Advances, 2015, 5, 76302-76308.	1.7	14
88	Ambient pressure dried graphene aerogels with superelasticity and multifunctionality. Journal of Materials Chemistry A, 2015, 3, 19268-19272.	5.2	125
89	Low-cost, flexible graphene/polyaniline nanocomposite paper as binder-free high-performance supercapacitor electrode. Functional Materials Letters, 2014, 07, 1440010.	0.7	5
90	One dimensional main-chain crystallization kinetics of poly(3-octylthiophenes) investigated by infrared spectroscopy. Vibrational Spectroscopy, 2014, 71, 1-5.	1.2	2

#	Article	IF	CITATIONS
91	Effect of a small amount of poly(3â€hydroxybutyrate) on the crystallization behavior of poly(<scp>l</scp> ″actic acid) in their immiscible and miscible blends during physical aging. Polymer International, 2014, 63, 1270-1277.	1.6	6
92	Solvent-Induced Crystallization Behaviors of PLLA Ultrathin Films Investigated by RAIR Spectroscopy and AFM Measurements. Journal of Physical Chemistry B, 2014, 118, 12652-12659.	1.2	23
93	A green and facile approach for the synthesis of water-dispersible reduced graphene oxide based on ionic liquids. Chemical Communications, 2014, 50, 2889-2892.	2.2	26
94	Tuning the Iridescence of Chiral Nematic Cellulose Nanocrystal Films with a Vacuum-Assisted Self-Assembly Technique. Biomacromolecules, 2014, 15, 4343-4350.	2.6	102
95	Chemical Structure and Interlayer Distance Correlation of Graphite Oxide in the Heating Process as Revealed by in Situ Fourier Transform Infrared Spectroscopy and Wide-Angle X-ray Diffraction Techniques. Applied Spectroscopy, 2014, 68, 570-576.	1.2	5
96	Fabrication of natural rubber nanocomposites with high graphene contents via vacuum-assisted self-assembly. RSC Advances, 2014, 4, 27687-27690.	1.7	38
97	The effect of poly(vinyl phenol) sublayer on the crystallization and melting behavior of poly(3-hydroxybutyrate) via hydrogen bonds. Polymer, 2014, 55, 5821-5828.	1.8	10
98	Tunable self-assembly structure of graphene oxide/cellulose nanocrystal hybrid films fabricated by vacuum filtration technique. RSC Advances, 2014, 4, 39301-39304.	1.7	35
99	Exfoliation and reduction of graphene oxide at low temperature and its resulting electrocapacitive properties. Journal of Materials Science, 2014, 49, 4989-4997.	1.7	16
100	Influence of crystal polymorphism on crystallinity calculation of poly(l-lactic acid) by infrared spectroscopy. Vibrational Spectroscopy, 2014, 70, 1-5.	1.2	23
101	Cold rystallization behavior of poly(<scp>L</scp> â€lactide)/ACR blend films investigated by <i>in situ</i> FTIR spectroscopy. Journal of Applied Polymer Science, 2013, 127, 4617-4623.	1.3	6
102	Effect of thermal annealing on the microstructure of P3HT thin film investigated by RAIR spectroscopy. Vibrational Spectroscopy, 2013, 68, 40-44.	1.2	17
103	Solvent-free preparation of polylactic acid fibers by melt electrospinning using umbrella-like spray head and alleviation of problematic thermal degradation. Journal of the Serbian Chemical Society, 2012, 77, 1071-1082.	0.4	30
104	Phase transition behavior of PLLA ultrathin film studied by grazing angle reflection absorption infrared spectroscopy. Vibrational Spectroscopy, 2012, 63, 338-341.	1.2	6
105	Tetrachloroperylene diimide functionalized reduced graphene oxide sheets and their l–V behavior by current sensing atomic force microscopy. Journal of Materials Chemistry, 2012, 22, 18839.	6.7	11
106	Charge and Pressure-Tuned Surface Patterning of Surfactant-Encapsulated Polyoxometalate Complexes at the Air–Water Interface. Langmuir, 2012, 28, 14624-14632.	1.6	18
107	Study on the Molecular Mobility in the Polyamide/SrFeO Composites by In Situ Infrared Spectroscopy. Journal of Macromolecular Science - Physics, 2012, 51, 1883-1891.	0.4	0
108	Spectroscopic analysis on cold drawing-induced PLLA mesophase. Polymer, 2012, 53, 4922-4926.	1.8	36

#	Article	IF	CITATIONS
109	Mapping mechanical properties of organic thin films by force-modulation microscopy in aqueous media. Beilstein Journal of Nanotechnology, 2012, 3, 464-474.	1.5	6
110	Synthesis of Dibenzothiophene ontaining Ladder Polysilsesquioxane as a Blue Phosphorescent Host Material. Chemistry - A European Journal, 2012, 18, 4115-4123.	1.7	37
111	Synthesis and Fluorescent Property of Pyrazoline Derivatives. Chinese Journal of Chemistry, 2012, 30, 1345-1350.	2.6	11
112	Mechanical properties and crystallization of Poly(L-lactide) films with several percents of ACR nanoparticles. Materials Letters, 2012, 83, 148-150.	1.3	9
113	Carbon nanotubes suppressed crystallization kinetics in PLLA thin film as revealed by in situ RAIR technique. Vibrational Spectroscopy, 2012, 61, 214-218.	1.2	5
114	Manipulating the Motion of Gold Aggregates Using Stimulusâ€Responsive Patterned Polymer Brushes as a Motor. Advanced Functional Materials, 2012, 22, 429-434.	7.8	17
115	Lamellar Orientation and Crystallization Dynamics of Poly (<scp>l</scp> -Lactic Acid) Thin Films Investigated by In-Situ Reflection Absorption Infrared Spectroscopy. Journal of Physical Chemistry B, 2011, 115, 11548-11553.	1.2	11
116	Effects of Intermolecular Hydrogen Bondings on Isothermal Crystallization Behavior of Polymer Blends of Cellulose Acetate Butyrate and Poly(3-hydroxybutyrate). Macromolecules, 2011, 44, 3467-3477.	2.2	33
117	Study on the Phase Transition Behavior of Poly(butylene adipate) in its Blends with Poly(vinyl phenol). Journal of Physical Chemistry B, 2011, 115, 1950-1957.	1.2	41
118	Effect of Solvent Evaporation Rate on Order-to-Disorder Phase Transition Behavior of Regioregular Poly(3-butylthiophene). Macromolecules, 2011, 44, 6128-6135.	2.2	30
119	Polymorphism and Structural Transition around 54 °C in Regioregular Poly(3-hexylthiophene) with High Crystallinity As Revealed by Infrared Spectroscopy. Macromolecules, 2011, 44, 9341-9350.	2.2	97
120	Physical Aging Enhanced Mesomorphic Structure in Melt-Quenched Poly(<scp> </scp> -lactic acid). Journal of Physical Chemistry B, 2011, 115, 13835-13841.	1.2	79
121	Isothermal crystallization behavior of water in poly(vinyl methyl ether) aqueous solution investigated by infrared and two-dimensional infrared correlation spectroscopy. Vibrational Spectroscopy, 2011, , .	1.2	2
122	Intermolecular interactions and crystallization behaviors of biodegradable polymer blends between poly (3-hydroxybutyrate) and cellulose acetate butyrate studied by DSC, FT-IR, and WAXD. Polymer, 2011, 52, 461-471.	1.8	51
123	Stimulus-responsive polymer brushes on surfaces: Transduction mechanisms and applications. Progress in Polymer Science, 2010, 35, 94-112.	11.8	348
124	Surfactant induced orientation of non-centrosymmetric polyoxometalate clusters in Langmuir–Blodgett films. Thin Solid Films, 2010, 519, 417-422.	0.8	6
125	Glass transition and disorder-to-order phase transition behavior of poly(l-lactic acid) revealed by infrared spectroscopy. Vibrational Spectroscopy, 2010, 53, 307-310.	1.2	35
126	PLLA Mesophase and Its Phase Transition Behavior in the PLLAâ^'PEGâ^'PLLA Copolymer As Revealed by Infrared Spectroscopy. Macromolecules, 2010, 43, 4240-4246.	2.2	111

#	Article	IF	CITATIONS
127	Melting Behavior of Epitaxially Crystallized Polycarprolactone on a Highly Oriented Polyethylene Thin Film Investigated by <i>in Situ</i> Synchrotron SAXS and Polarized Infrared Spectroscopy. Macromolecules, 2010, 43, 5315-5322.	2.2	20
128	A Study on the Epitaxial Ordering Process of the Polycaprolactone on the Highly Oriented Polyethylene Substrate. Macromolecules, 2010, 43, 362-366.	2.2	50
129	Fabrication of Micropatterned Stimulusâ€Responsive Polymerâ€Brush â€~Anemone'. Advanced Materials, 2009, 21, 1825-1829.	11.1	35
130	Crystallization, spherulite growth, and structure of blends of crystalline and amorphous poly(lactide)s. Polymer, 2009, 50, 4007-4017.	1.8	110
131	Molecular Orientation and Field-effect Transistors of a Rigid Rod Conjugated Polymer Thin Films. Journal of Physical Chemistry B, 2009, 113, 4176-4180.	1.2	34
132	Crystallization behavior of poly(l-lactic acid) affected by the addition of a small amount of poly(3-hydroxybutyrate). Polymer, 2008, 49, 4204-4210.	1.8	73
133	Disorder-to-Order Phase Transition and Multiple Melting Behavior of Poly(<scp>l</scp> -lactide) Investigated by Simultaneous Measurements of WAXD and DSC. Macromolecules, 2008, 41, 1352-1357.	2.2	737
134	Novel evaluation method of neutron reflectivity data applied to stimulus-responsive polymer brushes. Soft Matter, 2008, 4, 500.	1.2	21
135	Stereocomplexation and Monolayer Morphologies of a Stereoregular Poly(methyl methacrylate) Mixture Formed at the Air/Water Surface. Journal of Physical Chemistry C, 2007, 111, 6488-6494.	1.5	10
136	Investigation of Phase Transitional Behavior of Poly(l-lactide)/Poly(d-lactide) Blend Used to Prepare the Highly-Oriented Stereocomplex. Macromolecules, 2007, 40, 1049-1054.	2.2	217
137	Detailed interpretation of the results of two-dimensional correlation analysis of infrared spectra obtained during isothermal crystallization of isotactic polystyrene and poly(3-hydroxybutyrate). Vibrational Spectroscopy, 2007, 44, 50-55.	1.2	7
138	d-Poly(lactide) and LHRH decapeptide stereointeractions investigated by vibrational spectroscopy. European Polymer Journal, 2007, 43, 3016-3027.	2.6	8
139	Comparison of miscibility and structure of poly(3-hydroxybutyrate-co-3-hydroxyhexanoate)/poly(I-lactic acid) blends with those of poly(3-hydroxybutyrate)/poly(I-lactic acid) blends studied by wide angle X-ray diffraction, differential scanning calorimetry, and FTIR microspectroscopy, Polymer, 2007, 48, 1749-1755.	1.8	87
140	Multiple melting behavior of poly(3-hydroxybutyrate-co-3-hydroxyhexanoate) investigated by differential scanning calorimetryAandAinfrared spectroscopy. Polymer, 2007, 48, 4777-4785.	1.8	53
141	Câ~'H···OC Hydrogen Bonding and Isothermal Crystallization Kinetics of Poly(3-hydroxybutyrate) Investigated by Near-Infrared Spectroscopy. Macromolecules, 2006, 39, 3841-3847.	2.2	64
142	Crystal and Lamella Structure and Câ~'H··ÔC Hydrogen Bonding of Poly(3-hydroxyalkanoate) Studied by X-ray Diffraction and Infrared Spectroscopy. Macromolecules, 2006, 39, 1525-1531.	2.2	109
143	Crystallization Behaviors of Poly(3-hydroxybutyrate) and Poly(l-lactic acid) in Their Immiscible and Miscible Blends. Journal of Physical Chemistry B, 2006, 110, 24463-24471.	1.2	79
144	Molecular Weight Dependence of the Poly(l-lactide)/Poly(d-lactide) Stereocomplex at the Airâ^'Water Interface. Biomacromolecules, 2006, 7, 2728-2735.	2.6	31

#	Article	IF	CITATIONS
145	Epitaxial Crystallization of Isotactic Poly(Methyl Methacrylate) on Highly Oriented Polyethylene. Journal of Physical Chemistry B, 2006, 110, 738-742.	1.2	50
146	Surface-Induced Anisotropic Chain Ordering of Polycarprolactone on Oriented Polyethylene Substrate:  Epitaxy and Soft Epitaxy. Macromolecules, 2006, 39, 8041-8048.	2.2	73
147	Exploring Time-Dependent Structural Changes during the Cold Crystallization Process of Isotactic Polystyrene by Infrared Spectroscopy and Multivariate Curve Resolution. Applied Spectroscopy, 2006, 60, 155-161.	1.2	5
148	Confirmation of Disorderα Form of Poly(L-lactic acid) by the X-ray Fiber Pattern and Polarized IR/Raman Spectra Measured for Uniaxially-Oriented Samples. Macromolecular Symposia, 2006, 242, 274-278.	0.4	135
149	X-ray diffraction and infrared spectroscopy studies on crystal and lamellar structure and cho hydrogen bonding of biodegradable poly(hydroxyalkanoate). Macromolecular Research, 2006, 14, 408-415.	1.0	27
150	Raman microspectroscopy study of structure, dispersibility, and crystallinity of poly(hydroxybutyrate)/poly(l-lactic acid) blends. Polymer, 2006, 47, 3132-3140.	1.8	86
151	Structure characterization of melt drawn polyethylene ultrathin films. Science Bulletin, 2006, 51, 2844-2850.	1.7	13
152	Infrared Spectroscopy and X-Ray Diffraction Studies of CH…O Hydrogen Bonding and Thermal Behavior of Biodegradable Poly(hydroxyalkanoate). Macromolecular Symposia, 2005, 230, 158-166.	0.4	19
153	Differences in the CH3⋯OC interactions among poly(l-lactide), poly(l-lactide)/poly(d-lactide) stereocomplex, and poly(3-hydroxybutyrate) studied by infrared spectroscopy. Journal of Molecular Structure, 2005, 735-736, 249-257.	1.8	95
154	Miscibility and Hydrogen-Bonding Interactions in Biodegradable Polymer Blends of Poly(3-hydroxybutyrate) and a Partially Hydrolyzed Poly(vinyl alcohol). Journal of Physical Chemistry B, 2005, 109, 19175-19183.	1.2	45
155	Initial Crystallization Mechanism of Isotactic Polystyrene from Different States. Journal of Physical Chemistry B, 2005, 109, 5586-5591.	1.2	19
156	Crystal Modifications and Thermal Behavior of Poly(l-lactic acid) Revealed by Infrared Spectroscopy. Macromolecules, 2005, 38, 8012-8021.	2.2	775
157	Infrared Spectroscopic Study of CH3···OC Interaction during Poly(l-lactide)/Poly(d-lactide) Stereocomplex Formation. Macromolecules, 2005, 38, 1822-1828.	2.2	342
158	Structure, Dispersibility, and Crystallinity of Poly(hydroxybutyrate)/Poly(l-lactic acid) Blends Studied by FT-IR Microspectroscopy and Differential Scanning Calorimetry. Macromolecules, 2005, 38, 6445-6454.	2.2	233
159	Conformation Rearrangement and Molecular Dynamics of Poly(3-hydroxybutyrate) during the Melt-Crystallization Process Investigated by Infrared and Two-Dimensional Infrared Correlation Spectroscopy. Macromolecules, 2005, 38, 4274-4281.	2.2	120
160	Reflection-absorption infrared spectroscopy investigation of the crystallization kinetics of poly(ethylene terephthalate) ultrathin films. Journal of Polymer Science, Part B: Polymer Physics, 2004, 42, 4440-4447.	2.4	37
161	Class Transition Temperature Determination of Poly(ethylene terephthalate) Thin Films Using Reflectionâ^Absorption FTIR. Macromolecules, 2004, 37, 2532-2537.	2.2	70
162	Structure Changes during the Induction Period of Cold Crystallization of Isotactic Polystyrene Investigated by Infrared and Two-Dimensional Infrared Correlation Spectroscopy. Macromolecules, 2004, 37, 3292-3298.	2.2	44

#	Article	IF	CITATIONS
163	Structural Changes and Crystallization Dynamics of Poly(l-lactide) during the Cold-Crystallization Process Investigated by Infrared and Two-Dimensional Infrared Correlation Spectroscopy. Macromolecules, 2004, 37, 6433-6439.	2.2	257
164	Weak Intermolecular Interactions during the Melt Crystallization of Poly(l-lactide) Investigated by Two-Dimensional Infrared Correlation Spectroscopy. Journal of Physical Chemistry B, 2004, 108, 11514-11520.	1.2	173
165	Miscibility and phase structure of binary blends of polylactide and poly(vinylpyrrolidone). Journal of Applied Polymer Science, 2003, 88, 973-979.	1.3	60
166	Miscibility and phase structure of binary blends of polylactide and poly(methyl methacrylate). Journal of Polymer Science, Part B: Polymer Physics, 2003, 41, 23-30.	2.4	182
167	Novel transmittance change of polyelectrolyte hydrogel in DC electric field. Journal of Polymer Science, Part B: Polymer Physics, 2003, 41, 2290-2295.	2.4	4
168	Investigation of pH sensitivity of poly(acrylic acid-co-acrylamide) hydrogel. Polymer International, 2003, 52, 1153-1157.	1.6	44
169	Influence of the Interactions in Aqueous Mixtures of Poly(vinyl methyl ether) on the Crystallization Behavior of Water. Macromolecules, 2003, 36, 9145-9153.	2.2	29
170	Preparation of mesoporous MCM-41/poly(acrylic acid) composites using supercritical CO2 as a solvent. Journal of Materials Chemistry, 2003, 13, 1373.	6.7	16
171	In Situ FTIR Studies on the Cold-Crystallization Process and Multiple Melting Behavior of Isotactic Polystyrene. Macromolecules, 2003, 36, 4874-4879.	2.2	35
172	Frozen bound water melting induced cooperative hydration of poly(vinyl methyl ether) in aqueous solution. Polymer Bulletin, 2002, 48, 277-282.	1.7	22
173	Infrared spectroscopic study on the crystallization of water in poly(vinyl methyl ether) aqueous solution during heating. Journal of Polymer Science, Part B: Polymer Physics, 2002, 40, 2772-2779.	2.4	7